The Neural Bases of the Semantic Interference of Spatial Frequency-based Information in Scenes

Louise Kauffmann[1,2], Jessica Bourgin[1,2], Nathalie Guyader[1], and Carole Peyrin[1,2]

Abstract

■ Current models of visual perception suggest that during scene categorization, low spatial frequencies (LSF) are processed rapidly and activate plausible interpretations of visual input. This coarse analysis would then be used to guide subsequent processing of high spatial frequencies (HSF). The present fMRI study examined how processing of LSF may influence that of HSF by investigating the neural bases of the semantic interference effect. We used hybrid scenes as stimuli by combining LSF and HSF from two different scenes, and participants had to categorize the HSF scene. Categorization was impaired when LSF and HSF scenes were semantically dissimilar, suggesting that the LSF scene was processed automatically and interfered with categorization of the HSF scene. fMRI results revealed that this semantic interference effect was associated with increased activation in the inferior frontal gyrus, the superior parietal lobules, and the fusiform and parahippocampal gyri. Furthermore, a connectivity analysis (psychophysiological interaction) revealed that the semantic interference effect resulted in increasing connectivity between the right fusiform and the right inferior frontal gyri. Results support influential models suggesting that, during scene categorization, LSF information is processed rapidly in the pFC and activates plausible interpretations of the scene category. These coarse predictions would then initiate top–down influences on recognition-related areas of the inferotemporal cortex, and these could interfere with the categorization of HSF information in case of semantic dissimilarity to LSF. ■

INTRODUCTION

The human visual system is particularly efficient in processing and categorizing complex stimuli such as scenes (Thorpe, Fize, & Marlot, 1996). Convergent data on the functional neuroanatomy of visual pathways (Van Essen & Deyoe, 1995), neurophysiological recordings in primates (Shams & von der Malsburg, 2002; Hupé et al., 2001; De Valois, Albrecht, & Thorell, 1982; De Valois, Yund, & Hepler, 1982; Poggio, 1972; for a review, see Bullier, 2001), and psychophysical results in humans (Hughes, Nozawa, & Kitterle, 1996; Schyns & Oliva, 1994; Parker, Lishman, & Hughes, 1992; Ginsburg, 1986) support current models of visual perception (Kauffmann, Ramanoël, & Peyrin, 2014; Hegdé, 2008; Bar, 2003; Bullier, 2001; Schyns & Oliva, 1994), which suggest that visual analysis starts with the parallel extraction of different visual elementary features at different spatial frequencies. Low spatial frequencies (LSF) in scenes, conveyed by fast magnocellular pathways, provide coarse information about a visual stimulus (e.g., the global shape and structure of a scene), whereas high spatial frequencies (HSF) in scenes, conveyed more slowly by the parvocellular pathways, provide finer information about the stimulus (e.g., the edges and borders of an object in the scene).

On the basis of the neurophysiological properties of the magnocellular and parvocellular pathways, a number of studies using sinusoidal gratings (Hughes et al., 1996; Ginsburg, 1986) or scenes filtered in spatial frequency (Kauffmann, Chauvin, Guyader, & Peyrin, 2015; Musel, Chauvin, Guyader, Chokron, & Peyrin, 2012; Schyns & Oliva, 1994; Parker et al., 1992) as stimuli have shown temporal precedence of LSF over HSF processing in the time course of visual processing. Schyns and Oliva (1994), for example, used hybrid images made of two superimposed scenes belonging to different categories and containing different spatial frequency bands (e.g., a city scene in LSF superimposed with a highway scene in HSF). When exposure duration of hybrid images was very short (30 msec), perception of the hybrids was dominated by LSF information. However, when exposure duration was longer (150 msec), perception of the hybrids was dominated by HSF information. This suggests that scene perception follows a predominantly coarse-to-fine processing sequence, with a precedence of LSF processing over HSF processing.

Bar and colleagues (Bar, 2003, 2007; Kveraga, Boshyan, & Bar, 2007; Bar et al., 2006) proposed a proactive model for the cerebral mechanisms that may subserve visual recognition. According to this model, LSF information reaches the pFC rapidly and activates plausible semantic interpretations relating to the stimulus based on its coarse physical properties. The result of these predictions is then projected, via feedback connections, into the inferotemporal cortex (such as the fusiform and parahippocampal areas) to guide and facilitate subsequent

[1]Université Grenoble Alpes, [2]CNRS, Grenoble, France

processing of the finer HSF information conveyed more slowly through the ventral visual stream into the inferotemporal cortex. However, only a few studies have directly investigated the influence of LSF processing on subsequent HSF processing or the way in which LSF and HSF information integrate during scene categorization.

Mu and Li (2013), for example, investigated the neural correlates and time course of the integration of LSF and HSF information using ERP recordings during scene categorization. The authors presented hybrid scenes to participants who had to ignore the LSF component and perform a categorization task (man-made vs. natural) based only on the HSF component. On the basis of the assumption that a default coarse-to-fine processing occurs during scene categorization, the authors expected that the LSF component of the hybrid would be processed automatically and would influence the processing of HSF even if it was not relevant to performance of the task. For this purpose, they manipulated the semantic similarity between the LSF and HSF components of the hybrids. The two scenes of which the hybrids were made up were either semantically similar (e.g., LSF of a natural scene superimposed with HSF of another natural scene) or semantically dissimilar (e.g., LSF of a natural scene superimposed with HSF of a man-made scene). Participants made more categorization errors when hybrids were semantically dissimilar than when they were similar. This semantic interference effect revealed that the semantic information contained in the task-irrelevant LSF component was processed automatically and that it interfered with the categorization of the semantic information contained in HSF in the semantically dissimilar condition. In addition, the authors tested whether semantic interference could be modulated by the physical properties in scenes by manipulating the physical similarity (i.e., spatial overlap) between LSF and HSF. The two scenes composing the hybrid had either similar or dissimilar physical properties. Behavioral results showed that the semantic interference effect was greater when the two scenes composing the hybrids were physically similar. This result suggested that the spatial overlap of LSF on HSF caused even greater impairment of HSF categorization in the absence of any semantic congruence between the two scenes. On a neurobiological level, results from ERP recordings revealed that semantic interference was associated with a negative frontal component (N1) 122 msec after stimulus onset and that this component was greater when hybrids were physically similar than when they were physically dissimilar. The early frontal component associated with the semantic interference effect was followed by positive parietal and occipital components (P2 and P3) 247 and 344 msec after stimulus onset, respectively. In the context of the proactive model of visual perception (Bar, 2003, 2007; Bar et al., 2006), these results suggested that, when the LSF and HSF components of the hybrids were semantically dissimilar, coarse processing of LSF physical properties led to erroneous semantic predictions, resulting in greater bias in HSF categorization, and a more pronounced interference effect in frontal areas. Overall, these results suggested that processing of the semantic properties of LSF and HSF may occur in the early stages of visual processing in frontal areas, where it initiates top–down facilitation (Bar et al., 2006).

The aim of this study was to further examine, within the theoretical framework of coarse-to-fine scene categorization, how LSF in scenes may modulate and interfere with the processing of HSF by investigating, using fMRI, the neural bases of the semantic interference effect. As in the study by Mu and Li (2013), participants had to categorize hybrid scenes (man-made vs. natural) based on their HSF component and ignore the LSF component. We manipulated the semantic and physical similarity between LSF and HSF scenes composing the hybrids. The two scenes composing the hybrids were thus either (1) semantically and physically similar, (2) semantically similar and physically dissimilar, (3) semantically dissimilar and physically similar, or (4) semantically and physically dissimilar. On the basis of Mu and Li's (2013) results, we expected that categorization of the HSF component in the hybrids would be impaired when the LSF component was semantically dissimilar. Furthermore, we expected the semantic interference effect to be stronger when physical properties of the LSF and HSF components were similar than when they were dissimilar. At the cerebral level, we expected that the semantic interference effect would be associated mainly with activation of the pFC (Bar et al., 2006). Furthermore, according to Bar's proactive model of visual recognition, the pFC would influence processing of information in the fusiform gyrus. We therefore additionally performed a functional connectivity analysis (psychophysiological interaction, PPI) to examine whether connectivity between the fusiform gyrus and the pFC was influenced by the semantic similarity between LSF and HSF scenes in hybrids.

METHODS

Participants

Fourteen right-handed participants (two men; mean age = 24 years, *SD* = 7 years) with normal or corrected-to-normal vision and no history of neurological disorders were included in this experiment. All participants gave their informed written consent before participating in the study, which was in accordance with the Code of Ethics of the World Medical Association (Declaration of Helsinki) for experiments involving humans approved by the local ethics committee.

Stimuli and Procedure

Stimuli were constructed from 160 black and white photographs (256-level grayscales, 256 × 256 pixels) taken

among the 2687 scenes from the Labelme database (Oliva & Torralba, 2001). Scenes were classified into two distinct categories (80 natural scenes, e.g., forests, coasts, and open countryside, and 80 man-made scenes, e.g., highways, streets, and buildings) and subtended a visual angle of 6° × 6°.

Scenes were selected to obtain 40 scenes from each category with similar physical properties and 40 scenes from each category with dissimilar physical properties. Physical similarity of scenes was assessed using two criteria: the correlation between images based on their pixel intensity values (Image correlation) and the correlation between amplitude spectra of images (AS correlation, i.e., correlation between pixel intensity values of amplitude spectra, i.e., the module of the Fourier transform of images).

When considering the whole database (i.e., 2687 scenes), the mean Image correlation between all pairs of scenes in the database was 0.23 (SD = 0.26; ranging from −0.93 to 0.99) and the mean AS correlation was 0.52 (SD = 0.11; ranging from −0.08 to 0.98). Two scenes were considered physically similar if their Image correlation coefficient and AS correlation coefficient were superior to 0.6 (only 1.59% of images pairs matched both criteria). Two scenes were considered physically dissimilar if their Image correlation coefficient was inferior to 0.01 and their AS correlation coefficient was inferior to 0.6 (only 1.37% of image pairs matched both criteria). It should be noted that, overall, AS correlation coefficients were higher than Image correlation coefficients because of the similar 1/f shaped amplitude spectra, characteristic of natural scenes (Field, 1987). Mean correlation coefficients for physically similar (PS) and physically dissimilar (PD) conditions are shown in Table 1.

Each scene was filtered to preserve either LSF or HSF information, using the MATLAB image processing toolbox (The MathWorks, Inc., Sherborn, MA). Filtered scenes were obtained by multiplying the Fourier transform of the original images with Gaussian filters. The standard deviation of Gaussian filters was a function of the spatial frequency cutoff for a standard attenuation of 3 dB. We removed spatial frequency content above 2 cycles per degree of visual angle (i.e., 12 cycles per image) in LSF scenes and below 6 cycles per degree of visual angle (i.e., 36 cycles per image) in HSF scenes. The resulting filtered scenes were then normalized to obtain a mean luminance of 0.5, for luminance values between 0 and 1 (i.e., mean luminance of 128 on a gray-level scale). We then created hybrid stimuli by combining the LSF component in one scene with the HSF component in another scene. The two scenes that made up the hybrids could be either semantically similar (SS; e.g., LSF component of a natural scene superimposed with HSF component of another natural scene) or semantically dissimilar (SD; e.g., LSF component of a natural scene superimposed with HSF component of a man-made scene). Furthermore, the two scenes composing the hybrid could be either physically similar (PS) or physically dissimilar (PD). There were, therefore, four hybrid conditions (SS-PS, SS-PD, SD-PS, and SD-PD; see Figure 1) and, as a result, 160 hybrid stimuli (40 per hybrid condition). The HSF

Table 1. Mean (±SD) Image and AS Correlation between the Scenes Composing the Hybrids for Each Semantic and Physical Similarity Condition

	Semantically Similar		*Semantically Dissimilar*	
	Mean	±*SD*	*Mean*	±*SD*
Physically Similar				
Image correlation	0.75	±0.08	0.73	±0.06
AS correlation	0.67	±0.03	0.66	±0.04
Physically Dissimilar				
Image correlation	0.01	±0.00	0.01	±0.00
AS correlation	0.43	±0.06	0.44	±0.05

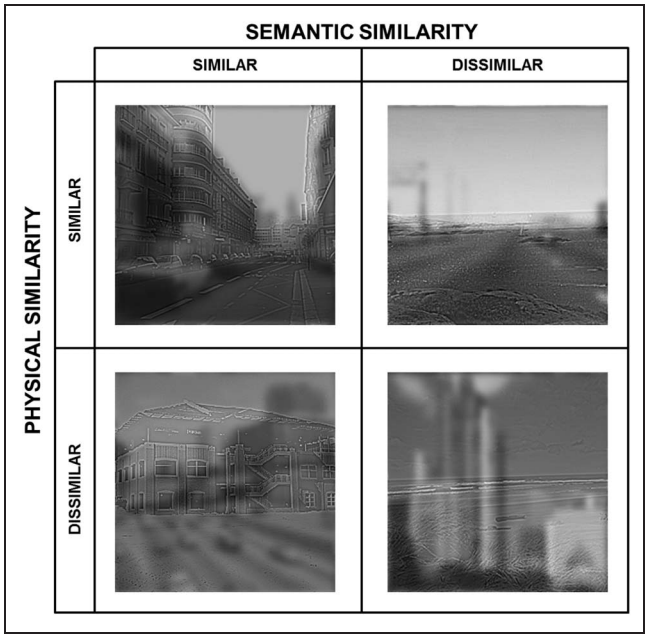

Figure 1. Example of hybrid stimuli from the two semantic similarity conditions and the two physical similarity conditions. The two scenes of which the hybrids were composed could be either (1) semantically and physically similar (e.g., LSF of a man-made scene superimposed with HSF of another man-made scene with similar physical properties), (2) semantically dissimilar and physically similar (e.g., LSF of a man-made scene superimposed with HSF of a natural scene with similar physical properties), (3) semantically similar and physically dissimilar (e.g., LSF of a man-made scene superimposed with HSF of another man-made scene with dissimilar physical properties), or (4) semantically and physically dissimilar (e.g., LSF of a man-made scene superimposed with HSF of a natural scene with dissimilar physical properties).

component of half of the hybrids in each experimental condition was that of a natural scene. The HSF component in the other half of the hybrids was that of a man-made scene. Stimuli were displayed using E-prime software (E-prime Psychology Software Tools, Inc., Pittsburgh, PA) and back-projected onto a translucent screen positioned at the rear of the magnet. Participants viewed this screen at a distance of about 222 cm via a mirror attached to the head coil. We used a backward mask, built with 1/*f* noise, to prevent retinal persistence of the scenes.

An event-related design paradigm was used. The experiment consisted of four functional runs. Each functional run lasted about 5 min and was composed of 95 events, including 80 hybrid events (20 per hybrid condition) and 15 null events (i.e., a black fixation dot displayed against a gray background). The order of hybrid conditions and null events was pseudorandomized based on an optimization algorithm (Friston, Zarahn, Josephs, Henson, & Dale, 1999). Each stimulus was displayed for 100 msec, followed by the mask (1/*f* noise) for 30 msec, and a fixation dot in the center of the screen. The interval between the onsets of two successive stimuli was 2.5 sec. Participants had to give a categorical answer based on the HSF components of the hybrids ("natural" or "man-made") by pressing the corresponding key with the forefinger and the middle finger of their dominant hand. They were instructed to fixate on the center of the screen (fixation dot) during the entire run and to respond as quickly and as accurately as possible by pressing one of two response keys. Half of the participants had to answer "natural" with their forefinger and "man-made" with the middle finger, whereas the second half of the participants had to answer "natural" with their middle finger and "man-made" with the forefinger. Response accuracy and RTs (in milliseconds) were recorded.

fMRI Acquisition

Experiments were performed using a whole-body 3T Philips scanner (Achieva 3.0T TX Philips, Philips Medical Systems, Best, NL) with a 32-channel head coil at the Grenoble MRI facility IRMaGe in France. For all functional scans, the manufacturer-provided gradient-echo/T2* weighted EPI method was used. Forty-four adjacent axial slices parallel to the bicommissural plane were acquired in sequential mode. Slice thickness was 3 mm. The in-plane voxel size was 2.5 × 2.5 mm (220 × 220 mm field of view acquired with a 88 × 85 pixel data matrix; reconstructed with zero filling to 96 × 96 pixels). The main sequence parameters were as follows: repetition time = 2.5 sec, echo time = 30 msec, flip angle = 80°. Finally, a T1-weighted high-resolution three-dimensional anatomical volume was acquired by using a 3-D T1 TFE sequence (field of view = 256 × 224 × 175 mm; resolution = 1.333 × 1.690 × 1.375 mm; acquisition matrix = 192 × 115 × 128 pixels; reconstruction matrix = 288 × 288 × 128 pixels).

Whole-brain Analysis

Data analysis was performed using the general linear model (Friston et al., 1995) for event-related designs in SPM8 (Wellcome Department of Imaging Neuroscience, London, UK, www.fil.ion.ucl.ac.uk/spm/) implemented in MATLAB 7. Individual scans were realigned, normalized to the Montreal Neurological Institute (MNI) space and spatially smoothed by an 8-mm FWHM Gaussian kernel. Time series for each voxel were high-pass filtered (1/128 Hz cutoff) to remove low-frequency noise and signal drift.

fMRI signal was analyzed using single-participant general linear model. For each participant, four conditions of interest (SS-PS, SS-PD; SD-PS, and SD-PD) were modeled as four regressors convolved with a canonical hemodynamic response function. Movement parameters derived from realignment corrections (three translations and three rotations), response accuracy, and RTs were also entered into the design matrix as additional factors of no interest to account for head motion-, accuracy-, and RT-related variance, respectively. Analyses were performed at the individual subject level to examine the contrasts between hybrid conditions. These contrast images were then entered into second-level random effect analyses to test for within group effects (one-sample *t* tests). The significance of activations was assessed with a statistical threshold of $p < .001$, uncorrected for multiple comparisons at the peak-level ($T > 3.85$, $k = 15$), and a threshold of $p < .05$, FWE-corrected at the cluster level.

Functional Connectivity Analysis

On the basis of Bar's proactive model of visual recognition (Bar et al., 2006; Bar, 2003) suggesting that LSF-based computations performed in the pFC influence processing of HSF information in the fusiform gyrus, we hypothesized that connectivity between these regions would be influenced by the semantic similarity between LSF and HSF scenes in hybrids. To address this question, we performed a PPI analysis. This approach allows to determine whether the connectivity between a seed region and all other voxels in the brain is affected by a psychological factor, such as the experimental conditions (Friston et al., 1997).

PPI analysis was performed using the standard procedure on SPM8. First, for each participant, seed regions were identified with a contrast in which all hybrids conditions were compared to the baseline. We used this contrast instead of the [SD > SS] contrast, because performing PPI analysis with a seed activated in the contrast of interest can lead to regressor collinearity and a lack of power. Indeed, in this latter case, the physiological and psychological variables would be correlated and would therefore also correlate with the PPI. Separate PPI analyses were performed for each seed region. In this study, the seed regions were the right and left fusiform gyrus. The choice of these seed regions was motivated by the

fact that (1) they were more easily identifiable at the individual level than the inferior frontal gyrus, which could not be identified in each participant at the statistical threshold used ($p < .05$), and (2) they showed less variability in individual activation peak coordinates than the inferior frontal gyrus, which peak coordinates varied more between participants. The physiological activity of each seed region was computed by extracting time series (i.e., principal component adjusted for effects of interest and BOLD deconvolved to get an estimate of the neural response; Gitelman, Penny, Ashburner, & Friston, 2003) of all voxels within 4-mm spheres centered on subject-specific maxima (identified at a threshold of $p < .05$, uncorrected) closest to the group activation peak (identified at a threshold of $p < .001$, uncorrected) of the left and right fusiform gyri (mean Talairach coordinates ± *SD*): left fusiform gyrus, $x = -26 \pm 5, y = -42 \pm 5, z = -10 \pm 3$; right fusiform gyrus, $x = -27 \pm 4, y = -45 \pm 6, z = -13 \pm 4$. The semantic interference effect (i.e., [SD > SS] contrast) was used to compute the psychological factor hypothesized to influence connectivity. Finally, the PPI variable representing the interaction between the physiological and psychological factors was computed. For each participant, a new first-level general linear model was created for each PPI analysis, including the PPI, physiological, and psychological variables as regressors of interest convolved with the canonical hemodynamic response function. RT and accuracy were also modeled as regressors of no interest (O'Reilly, Woolrich, Behrens, Smith, & Johansen-Berg, 2012). Analyses were performed at the individual level to examine the effect of the PPI term. These contrast images were then entered into second-level random effect analyses to test for within group effects (one-sample *t* tests). This produced statistical parametric maps revealing voxels with significant positive connectivity with the seed regions because of the semantic dissimilarity between LSF and HSF scenes in hybrids. The significance of activations was assessed with a statistical threshold of $p < .001$, uncorrected for multiple comparisons at the peak level ($T > 3.85$, $k = 5$).

For the whole-brain and PPI analyses, a transformation of MNI into Talairach and Tournoux (1988) coordinates was performed using the MNI2TAL function (created by Matthew Brett, available at www.mrc-cbu.cam.ac.uk/Imaging) to facilitate comparison with other studies.

RESULTS

Behavioral Results

Two 2 × 2 ANOVAs with Semantic similarity (SS and SD) and Physical similarity (PS and PD) as within-subject factors were conducted on mean error rates and mean correct RTs (see Figure 2).

The ANOVA conducted on mean error rates revealed a main effect of Semantic similarity ($F(1, 13) = 51.52$, $p < .001$, $\eta^2_p = 0.798$). Participants made more errors when categorizing the hybrids in the SD condition (mean ± *SE*: 34.69 ± 3.14%) than in the SS condition (9.73 ± 1.46%), suggesting that the semantic information of the LSF component interfered with the processing of the semantic information of HSF component. There was no main effect of Physical similarity (PS: 22.59 ± 2.01%; PD: 21.83 ± 1.73%; $F(1, 13) < 1$, $\eta^2_p = 0.019$). The expected interaction between Semantic similarity and Physical similarity was not significant ($F(1, 13) = 2.59$, $p = .13$, $\eta^2_p = 0.166$).

The ANOVA conducted on mean correct RTs revealed a main effect of Semantic similarity ($F(1, 13) = 23.17$, $p < .001$, $\eta^2_p = 0.641$). Participants categorized the hybrids more rapidly in the SS condition (795 ± 29.46 msec) than in the SD condition (868 ± 33.15 msec). As for the analysis on mean error rates, this semantic interference effect indicated that the processing of the LSF component interfered with the processing of the HSF component at the semantic level. There was no effect of physical similarity (PS: 840 ± 33.50 msec; PD: 822 ± 27.95 msec; $F(1, 13) = 3.30$, $p = .09$, $\eta^2_p = 0.202$). The expected interaction between semantic similarity and physical similarity was not significant ($F(1, 13) < 1$ $\eta^2_p = 0.002$).

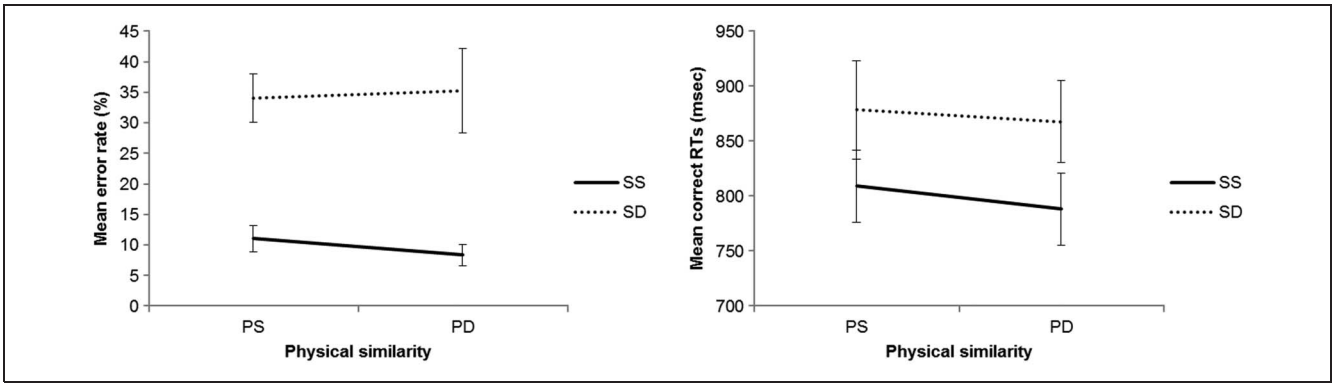

Figure 2. Mean error rates (%) and mean correct RTs (msec) for the categorization of hybrids, according to semantic similarity (semantically similar [SS] and semantically dissimilar [SD]) and physical similarity (physically similar [PS] and physically dissimilar [PD]) between the two scenes composing the hybrids. Error bars indicate standard error.

fMRI Results

Whole-brain Results

We examined the regions specifically involved by the semantic interference effect of LSF on HSF processing by contrasting activations elicited by hybrids in the SD condition to activations elicited by hybrids in the SS condition ([SD > SS] contrast, cf. Figure 3). Results revealed that the semantic interference effect involved more strongly temporal, parietal, and frontal areas (cf. Table 2). Temporal activations corresponded to the bilateral fusiform gyri (BA 20/37), parahippocampal gyri (BA 37), and the right inferior temporal gyrus (BA 37). Occipito-parietal activations involved bilaterally the superior parietal lobules (BA 7) and the superior occipital gyrus (i.e., occipito-parietal junction) extending to the middle occipital gyrus in the right hemisphere. Finally, frontal activation involved the left medial and superior frontal gyrus (BA 8) including the SMA (BA 6) and the bilateral inferior frontal gyri (AB 45/46) extending to the OFC (BA 47) in the right hemisphere. The reverse contrast ([SS > SD]) revealed stronger activation of the bilateral superior frontal gyri (BA 10), the left posterior cingular gyrus (BA 31), and the left middle temporal gyrus (BA 39).

Although it was not the main interest of the study, we also tested the effect of physical similarity between scenes in hybrids by contrasting activations between the physically similar and dissimilar conditions. The [PD > PS] contrast revealed that physical dissimilarity between scenes in hybrids resulted in greater activation of occipito-temporal areas, including the bilateral lingual gyrus (BA 17/18), the bilateral cuneus (BA 19), the right inferior occipital gyrus (BA 18/19), the left middle occipital gyrus (BA 19/20), and the right superior temporal gyrus (BA 42). The reverse contrast ([PS > PD]) was not significant. Finally, the interaction between the semantic and physical similarity of scenes in hybrids was not significant.

Functional Connectivity Results

PPI for the semantic interference effect revealed stronger functional connectivity between the right parahippocampal gyrus and the right inferior frontal gyrus (BA 44, k = 19, peak coordinates: x = 39, y = 16, z = 11; t = 5.21; BA 45, k = 10, peak coordinates: x = 39, y = 28, z = 16; t = 5.05; Figure 3B) in the SD condition than in the SS condition. Importantly, this activation cluster overlapped with the activation of the inferior frontal gyrus observed with the [SD > SS] contrast in the whole-brain analysis (cf. Figure 3C). The PPI analysis using the left fusiform gyrus as seed region did not reveal any significant activation.

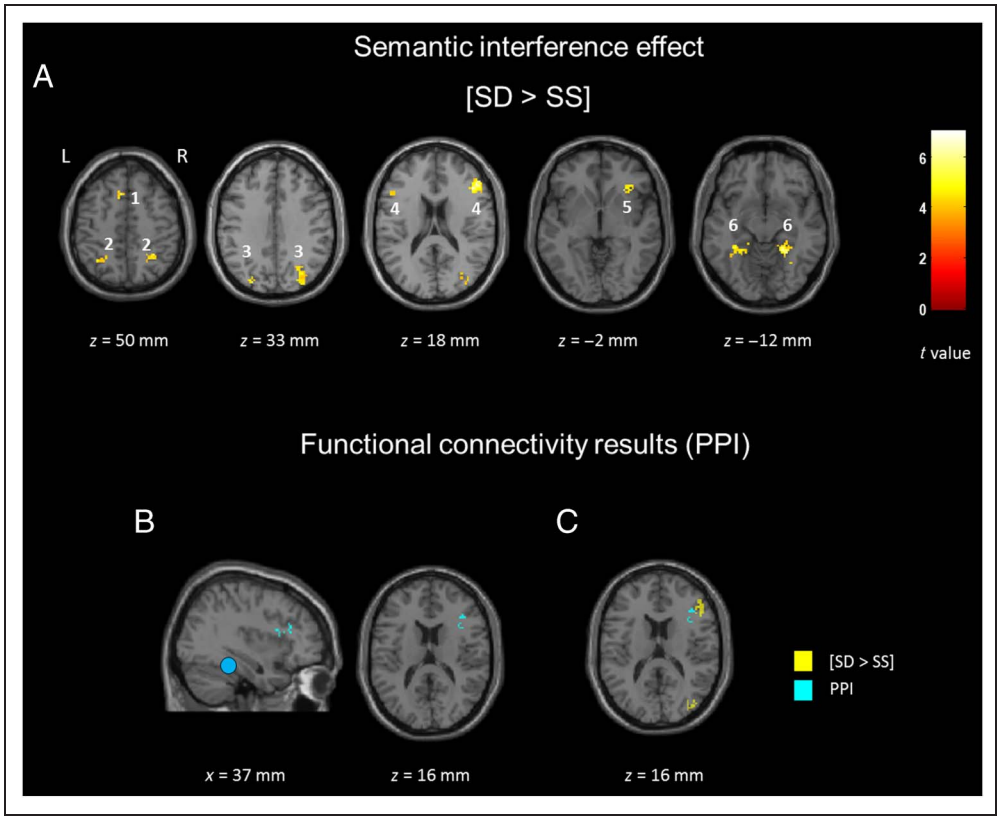

Figure 3. (A) Activations elicited by the semantic interference effect ([SD > SS] contrast): (1) the superior frontal gyrus, (2) the superior parietal lobules, (3) the superior/middle occipital gyri, (4) the inferior frontal gyri, (5) the OFC, and (6) the parahippocampal and fusiform gyri. Activations are reported at a statistical threshold of p < .001 uncorrected for multiple comparisons at the cluster level and a threshold of p < .05 FEW-corrected at the peak-level. (B) Region (right inferior frontal gyrus) showing increased connectivity with the right fusiform gyrus (blue circle) during the semantic interference effect, identified with the PPI analysis. (C) Superposition of clusters activated for the semantic interference effect ([SD > SS] contrast, in yellow) and clusters showing increase in connectivity with the parahippocampal gyrus for the semantic interference effect (PPI analysis, in blue).

Table 2. Cerebral Regions Specifically Activated for the Semantic Interference Effect ([SD > SS] and [SS > SD] Contrasts)

	Side	*BA*	*k*	*x*	*y*	*z*	*t*
Semantic Interference Effect							
[SD > SS]							
Temporal areas							
Parahippocampal gyrus	R	19	136	24	−46	−4	6.63
[Fusiform gyrus]		37		29	−54	−12	6.10
Parahippocampal gyrus	L	37	91	−33	−39	−10	5.56
[Fusiform gyrus]		20		−32	−37	−15	5.45
[Fusiform gyrus]		37		−23	−44	−10	5.33
Occipito-parietal areas							
Superior parietal lobule	R	7	58	37	−50	53	6.57
Superior parietal lobule	L	7	15	−23	−60	54	5.17
Superior occipital gyrus	R	19	207	29	−71	29	6.98
[Middle occipital gyrus]	R	18/19		42	−82	8	6.02
[Inferior parietal lobule]		40		32	−65	40	4.55
Superior occipital gyrus	L	19	29	−25	−78	35	5.77
Frontal areas							
Inferior frontal gyrus	R	45	116	49	33	16	7.01
Orbitofrontal cortex	R	47	47	29	25	−3	6.07
[Inferior frontal gyrus]	R	45/47		37	32	2	5.73
Inferior frontal gyrus	L	44	23	−40	4	26	5.36
			31	−50	21	25	4.83
Medial frontal gyrus	L	6	36	−8	17	47	5.75
[Superior frontal gyrus]		6		−10	10	53	4.92
[SS > SD]							
Superior frontal gyrus	L	10	111	−5	61	−2	6.48
[Superior frontal gyrus]	R	10		2	64	0	5.26
Cingular gyrus	L	31	27	−8	−39	39	6.14
Middle temporal gyrus	L	39	21	−60	−9	4	5.23
Physical Interference Effect							
[PD > PS]							
Lingual gyrus	L	17/18	592	−15	−87	0	6.77
[Lingual gyrus]	R	17/18		17	−82	−5	6.43
[Inferior occipital gyrus]	R	18/19		37	−75	−5	5.73
Cuneus	R/L	19	24	0	−85	30	5.86
Cuneus	R	19	33	24	−86	27	5.71

Table 2. (*continued*)

	Side	*BA*	*k*	*x*	*y*	*z*	*t*
Middle occipital gyrus	L	19/20	34	−43	−77	10	5.73
Superior temporal gyrus	R	42	50	44	−33	11	5.26
[PS > PD]							
No significant cluster							

For each cluster, the region showing the maximum t value is listed first, followed by the other regions in the cluster [in brackets]. Talairach coordinates (x, y, z) are indicated. R = right hemisphere; L = left hemisphere; BA = Brodmann's area; k = number of voxels in the cluster. Activations are reported at a statistical threshold of $p < .001$, uncorrected for multiple comparisons, and a minimum cluster size of $k = 15$ voxels.

DISCUSSION

Influential models of visual perception (Kauffmann et al., 2014; Hegdé, 2008; Bar, 2003; Bar et al., 2006; Schyns & Oliva, 1994) postulate that, during scene categorization, LSF are processed earlier than HSF (coarse-to-fine processing sequence). This initial low-pass analysis would be used to generate predictions about the nature of the visual input and facilitate the subsequent processing of HSF information (Bar, 2003, 2007; Bar et al., 2006). The aim of the present fMRI study was to gain better understanding of how the processing of LSF may modulate and interfere with the processing of HSF by investigating the neural bases of the semantic interference effect using fMRI and within the theoretical framework of the coarse-to-fine categorization of scenes.

On a behavioral level, we observed that the categorization of HSF scenes in hybrids was impaired when the LSF scene was semantically dissimilar. This result replicates the previous findings of Mu and Li (2013) and indicates that, although it was not relevant to the task, the nonattended categorical information from LSF was processed automatically and interfered with the processing of the task-relevant HSF semantic information. This semantic interference effect could be interpreted in the context of the proactive model of visual perception proposed by Bar et al. (Bar, 2003, 2007; Bar et al., 2006). In this model, coarse information from LSF is used to generate predictions about the visual input, and guides subsequent processing of HSF. Therefore, in the semantically dissimilar condition, the rapid processing of the LSF scene in the hybrid could have led to erroneous semantic predictions for the categorization of the HSF scene, resulting in an increase in error rates and RT for the correct categorization of HSF information. However, unlike Mu and Li (2013), we did not find that the semantic interference effect was modulated by the physical similarity between HSF and LSF scenes in hybrids. It should be noted that, in this study, RTs were longer overall (800–1000 msec) than those reported in the Mu and Li (2013) study (under 800 msec). This may have been due to greater physical constraints during the fMRI experiment (i.e., participants had to adopt a lying-down position in the magnet and were instructed not to move). These methodological differences may have prevented us from detecting any modulation of the semantic interference effect by the physical similarity of the scenes in RTs.

On a neurobiological level, fMRI results supported Mu and Li's (2013) EEG results, as they revealed that the semantic interference effect ([SD > SS] contrast) was associated with greater activation in specific areas of the frontal, parietal, and temporal cortices. However, our fMRI results did not reveal significant interaction between the semantic and physical similarity of scenes in hybrids.

As expected, in the frontal cortex, the semantic interference effect was associated with the bilateral activation of the inferior frontal gyrus, extending to the right OFC. These regions of the pFC are thought to be particularly involved in tasks requiring the retrieval of semantic information related to visual stimuli (Badre, Poldrack, Paré-Blagoev, Insler, & Wagner, 2005; Freedman, Riesenhuber, Poggio, & Miller, 2001; Wagner, Pare, Clark, & Poldrack, 2001). They also contribute to the maintenance of visual information in visual awareness or working memory (Fletcher & Henson, 2001). Activation of the inferior frontal gyrus therefore seems consistent with the categorization task demands in the semantically dissimilar (SD) condition, which involved the semantic processing of different visual information. This result can be linked to Mu and Li's (2013) ERP results showing a frontal N1 component associated with the semantic interference effect. However, these authors observed that this component was greater in case of physical similarity between the scenes in hybrids only. In their study, this N1 component was observed very early on, 120 msec after stimulus onset, suggesting that frontal areas were involved in the semantic processing of spatial frequencies in the early stages of visual processing. The involvement of the inferior frontal gyrus during rapid scene categorization was also evidenced in a combined fMRI and ERP study conducted by Peyrin et al. (2010). In that study, the authors showed that the successive processing of an LSF scene followed by an HSF scene resulted in both greater fMRI activation and greater ERP source activity (150–194 msec after the onset of the LSF scene) in the inferior frontal gyrus. These findings suggest that the greater activation of the inferior

frontal gyrus in the semantically dissimilar condition may be linked to the rapid processing of LSF information in scenes. Overall, the greater activation of the inferior frontal gyrus associated with the semantic interference effect in this study, together with findings from previous studies (Mu & Li, 2013; Peyrin et al., 2010), are consistent with the proactive model of visual recognition proposed by Bar and colleagues (Bar, 2003, 2007; Bar et al., 2006). According to this model, semantic predictions performed on the basis of LSF information occur very early in the inferior frontal gyrus (in the OFC) and initiate top–down facilitation to guide subsequent processing of HSF. As previously mentioned, in our semantically dissimilar condition, the rapid processing of the LSF scene could have led to erroneous semantic predictions (as suggested by the increased error rates in Behavioral Results), which may have resulted in increased activity in the inferior frontal gyrus. Our results therefore provide a new argument in favor of the involvement of the inferior frontal gyrus in processing the semantic properties of spatial frequency information. It can be noted that activation of the inferior frontal gyrus and mainly the OFC appears to be slightly right-lateralized. Interestingly, a recent fMRI study (Fintzi & Mahon, 2013) demonstrated that the right OFC responds more strongly to the LSF components in a coarse-to-fine sequence processing of objects, whereas the left OFC responds more strongly to the medium spatial frequency and HSF components. As previously suggested, categorization of the HSF scenes in the semantically dissimilar hybrid condition was interfered by the processing of the incongruent semantic information of the LSF scenes. The right OFC could thus have been more sensitive to the incongruent semantic information contained in LSF.

Additional frontal cortex activation was observed in the left superior frontal gyrus, including the SMA (BA 8/6), when the two scenes were semantically dissimilar (compared to the semantically similar condition). These regions have been shown to be involved when conflict between alternative motor responses occurs, as is the case in go/no-go tasks (e.g., Garavan, Ross, Kaufman, & Stein, 2003; Garavan, Ross, Murphy, Roche, & Stein, 2002), and activity in this region increases with increasing uncertainty in decision-making (Volz, Schubotz, & von Cramon, 2005). Stronger activation of this region in the semantically dissimilar condition, in which the incongruent category of the LSF scene interfered with the response to the HSF scene, could therefore reflect increased uncertainty and greater conflict between the motor responses to the HSF scene category.

In the parietal cortex, the semantic interference effect was associated with activation of the right occipito-parietal junctions. Activation of the right occipito-parietal junction has been observed previously in tasks requiring category-matching between two scenes (Peyrin et al., 2005), which may be consistent with our task involving the simultaneous processing of two different scenes. We also observed greater activation of the superior parietal lobules associated with the semantic interference effect. Involvement of these regions has previously been shown in tasks requiring high levels of attention (Peyrin et al., 2010; Behrmann, Geng, & Shomstein, 2004; Posner & Petersen, 1990) and attentional selection of relevant visual information (Capotosto et al., 2013; Shomstein, 2012; Yantis et al., 2002) or spatial frequency content (Baumgartner et al., 2013; Peyrin et al., 2010; Peyrin, Baciu, Segebarth, & Marendaz, 2004) to perform a visual task. The superior parietal lobule in particular appears to be predominantly involved in the top–down, task-driven, allocation of attention (Shomstein, 2012; Corbetta & Shulman, 2002; Yantis et al., 2002). Greater activation of this region in the semantically dissimilar condition could therefore reflect the use of greater attentional resources (as suggested by the increased error rate and RTs in that condition; see Behavioral Results), leading to an intensive recruitment of this parietal structure to allocate attention to the relevant spatial frequency information needed to perform the task.

Finally, in the occipito-temporal cortex, the semantic interference effect was associated with activation of the fusiform and parahippocampal gyri. The fusiform gyrus is known to be involved in object recognition (Grill-Spector, 2003; Haxby et al., 2001; Lerner, Hendler, Ben-Bashat, Harel, & Malach, 2001; Ishai, Ungerleider, Martrin, Schouten, & Haxby, 1999; Tanaka, 1996). Activation in the parahippocampal gyrus overlaps with activation in the parahippocampal place area, which has been shown to be predominantly and selectively involved in scene perception and recognition (Epstein, Harris, Stanley, & Kanwisher, 1999; Epstein & Kanwisher, 1998). Importantly, the fusiform and parahippocampal gyri both play a central role in Bar's model of visual recognition (Bar, 2003, 2007; Bar et al., 2006). In this model, these regions of the inferotemporal cortex combine top–down LSF-based semantic predictions from frontal areas with bottom–up HSF information from the ventral visual stream to enable recognition. In that theoretical context, greater activation of these regions in the SD condition (compared to in the SS condition) could therefore be explained by a conflict between (1) top–down predictions based on the LSF component in hybrids and (2) the bottom–up processing of HSF information.

Results of this study may raise the question of the interactions between regions involved in the semantic interference effect. In their study, Mu and Li (2013) showed that the first ERP component associated with the semantic interference effect occurred in frontal areas, followed by ERP components in parietal and occipital areas. According to these authors, this first ERP component indicated that information from both LSF and HSF was rapidly processed on a semantic level in frontal areas. Although this appears to be in disagreement with Bar's assumption (Bar, 2003, 2007; Bar et al., 2006) that only LSF information is rapidly processed in inferior frontal areas, the authors suggested that the demands of the task, which involved focusing the attention on HSF information, may have resulted in the enhancement of HSF perception and processing speed (Abrams, Barbot, &

Carrasco, 2010; Carrasco & Mcelree, 2001; Oliva & Schyns, 1997), enabling rapid processing of that information in inferior frontal areas. The semantic processing of LSF and HSF scenes in inferior frontal areas would have then initiated top–down influences to parieto-temporal areas to facilitate subsequent perceptual analyses and allow the categorization task to be accomplished. However, because our fMRI results do not provide any information about the time course of activation, one possible alternative interpretation is that the greater activation of the inferior frontal gyrus associated with the semantic interference effect seen in this study results from changes in connectivity with other regions, such as the parahippocampal place area and fusiform gyrus. It is possible that, in the semantically dissimilar condition, for example, inferior frontal and occipito-temporal regions involved in the processing of visual scene information interacted more strongly to disambiguate and enhance/inhibit processing of task-relevant/-irrelevant spatial frequency information.

To address whether connectivity between the inferior frontal gyrus and inferotemporal gyrus was modulated by the semantic interference effect, we conducted a functional connectivity analysis using PPI. The left and right fusiform gyri were defined as seed regions. Our results revealed that the semantic interference effect resulted in increasing connectivity between the right fusiform and right inferior frontal gyri. Thus, these results seem consistent with Bar's model of visual recognition (Bar, 2003, 2007; Bar et al., 2006) suggesting functional connectivity between the pFC and the fusiform gyrus and support our proposal that these regions interacted more strongly in case of semantic dissimilarity between LSF and HSF scenes in hybrids. It should however be noted that the PPI method does not allow determining of the direction of interactions between regions and only informs about regions which activity correlates with the one of the seed region, according to the experimental context. Therefore, it did not allow us to clarify which region influences the other.

Increase in functional coupling between inferotemporal areas and the inferior frontal gyrus in the context of an interference effect was supported by the results of a recent fMRI study (Wais, Rubens, Boccanfuso, & Gazzaley, 2010) investigating the interference effect of irrelevant visual information (a visual scene) on a concurrent process (the recollection of objects) involving mental imagery. Firstly, results showed that the recollection process was associated with activation of the inferior frontal gyrus, the hippocampus, and the visual association cortex and that this connectivity network was diminished when a visual stimulation interfered with the recollection process. This interference effect by a visual scene was associated with greater activation of the parahippocampal gyrus, and when the interference led to recollection errors, connectivity between the inferior frontal gyrus and the parahippocampal gyrus increased. The authors hypothesized that their results could reflect an overwhelming influence of a bottom–up processing of the interfering visual information. This would result in the inferior frontal gyrus being excluded from involvement in the recollection task to control and minimize these interfering influences. This would mean that in the last case the inferior frontal gyrus was involved in the cognitive control of task-relevant information processing (see also Nelson, Reuter-Lorenz, Persson, Sylvester, & Jonides, 2009; Chong, Williams, Cunnington, & Mattingley, 2008). Importantly, the inferior frontal gyrus has also been reported in a large number of studies implicating response conflict tasks as monitoring response conflict resolution (e.g., in Stroop tasks or go/no-go tasks; see Nee, Wager, & Jonides, 2007, for a meta-analysis). It is thus possible that, in this study, greater activation of the inferior frontal gyrus for the semantic interference effect also reflect such management of response conflict. Unfortunately, the design used here does not allow us to dissociate the effects of semantic similarity from the effects of response conflict resolution since these factors were confounded.

To conclude, results of this study provide additional support for influential models of visual perception (Peyrin et al., 2010; Bar, 2003, 2007; Bar et al., 2006; Schyns & Oliva, 1994), which suggest that LSF information in scenes is processed automatically and rapidly on a semantic level—in keeping with the coarse-to-fine hypothesis—and modulates subsequent processing of HSF information. On the basis of previous studies (Mu & Li, 2013; Peyrin et al., 2010; Bar et al., 2006), we propose that, during scene categorization, information from LSF may be rapidly processed in the inferior frontal gyrus to activate plausible interpretations of the scene category. These coarse predictions may then initiate top–down influences on recognition-related areas of the inferotemporal cortex and thus could interfere with the categorization of HSF information in the case of semantic dissimilarity between LSF and HSF. This may result in greater interactions between frontal and inferotemporal areas to disambiguate between LSF and HSF inconsistent information. During the categorization process, the parietal cortex may also be recruited to constrain the allocation of attention to the relevant visual information.

Acknowledgments

This work was supported by the RECOR ANR grant (ANR-12-JHS2-0002-01 RECOR) and a subvention from "Grenoble Pôle Cognition." Louise Kauffmann was supported by Région Rhône-Alpes (Cible Grants). The Grenoble MRI facility IRMaGe was partly funded by the French program "Investissement d'Avenir" run by the "Agence Nationale pour la Recherche": Grant "Infrastructure d'Avenir en Biologie Santé" (ANR-11-INBS-0006). We thank Catherine Dal Molin for the English revision of the manuscript.

Reprint requests should be sent to Louise Kauffmann, Université Grenoble Alpes, LPNC, Université Pierre Mendès France, BP 47, 38040 Grenoble Cedex09, France, or via e-mail: louise.kauffmann@upmf-grenoble.fr.

REFERENCES

Abrams, J., Barbot, A., & Carrasco, M. (2010). Voluntary attention increases perceived spatial frequency. *Attention, Perception & Psychophysics, 72,* 1510–1521.

Badre, D., Poldrack, R. A., Paré-Blagoev, E. J., Insler, R. Z., & Wagner, A. D. (2005). Dissociable controlled retrieval and generalized selection mechanisms in ventrolateral prefrontal cortex. *Neuron, 47,* 907–918.

Bar, M. (2003). A cortical mechanism for triggering top–down facilitation in visual object recognition. *Journal of Cognitive Neuroscience, 15,* 600–609.

Bar, M. (2007). The proactive brain: Using analogies and associations to generate predictions. *Trends in Cognitive Sciences, 11,* 280–289.

Bar, M., Kassam, K. S., Ghuman, A. S., Boshyan, J., Schmid, A. M., Dale, A. M., et al. (2006). Top–down facilitation of visual recognition. *Proceedings of the National Academy of Sciences, U.S.A., 103,* 449–454.

Baumgartner, F., Hanke, M., Geringswald, F., Zinke, W., Speck, O., & Pollmann, S. (2013). Evidence for feature binding in the superior parietal lobule. *Neuroimage, 68,* 173–180.

Behrmann, M., Geng, J. J., & Shomstein, S. (2004). Parietal cortex and attention. *Current Opinion in Neurobiology, 14,* 212–217.

Bullier, J. (2001). Integrated model of visual processing. *Brain Research, 36,* 96–107.

Capotosto, P., Tosoni, A., Spadone, S., Sestieri, C., Perrucci, M. G., Romani, G. L., et al. (2013). Anatomical segregation of visual selection mechanisms in human parietal cortex. *Journal of Neuroscience, 33,* 6225–6229.

Carrasco, M., & Mcelree, B. (2001). Covert attention accelerates the rate of visual information processing. *Proceedings of the National Academy of Sciences, 98,* 5363–5367.

Chong, T. T.-J., Williams, M. A., Cunnington, R., & Mattingley, J. B. (2008). Selective attention modulates inferior frontal gyrus activity during action observation. *Neuroimage, 40,* 298–307.

Corbetta, M., & Shulman, G. L. (2002). Control of goal-directed and stimulus-driven attention in the brain. *Nature Reviews Neuroscience, 3,* 201–215.

De Valois, R., Albrecht, D., & Thorell, L. (1982). Spatial frequency selectivity of cells in macaque visual cortex. *Vision Research, 22,* 545–559.

De Valois, R., Yund, W., & Hepler, N. (1982). The orientation and direction selectivity of cells in macaque visual cortex. *Vision Research, 22,* 531–544.

Epstein, R., Harris, A., Stanley, D., & Kanwisher, N. (1999). The parahippocampal place area: Recognition, navigation, or encoding? *Neuron, 23,* 115–125.

Epstein, R., & Kanwisher, N. (1998). A cortical representation of the local visual environment. *Nature, 392,* 598–601.

Field, D. J. (1987). Relations between the statistics of natural images and the response properties of cortical cells. *Journal of the Optical Society of America, 4,* 2379–2394.

Fintzi, A. R., & Mahon, B. Z. (2013). A bimodal tuning curve for spatial frequency across left and right human orbital frontal cortex during object recognition. *Cerebral Cortex, 24,* 1311–1318.

Fletcher, P. C., & Henson, R. N. A. (2001). Frontal lobes and human memory: Insights from functional neuroimaging. *Brain, 124,* 849–881.

Freedman, D. J., Riesenhuber, M., Poggio, T., & Miller, E. K. (2001). Categorical representation of visual stimuli in the primate prefrontal cortex. *Science, 291,* 312–316.

Friston, K. J., Buechel, C., Fink, G. R., Morris, J., Rolls, E., & Dolan, R. J. (1997). Psychophysiological and modulatory interactions in neuroimaging. *Neuroimage, 6,* 218–229.

Friston, K. J., Holmes, A. P., Worsley, K. J., Poline, J. P., Frith, C. D., & Frackowiak, R. S. (1995). Statistical parametric maps in functional imaging: A general linear approach. *Human Brain Mapping, 2,* 189–210.

Friston, K. J., Zarahn, E., Josephs, O., Henson, R. N., & Dale, A. M. (1999). Stochastic designs in event-related fMRI. *Neuroimage, 10,* 607–619.

Garavan, H., Ross, T. J., Kaufman, J., & Stein, E. A. (2003). A midline dissociation between error-processing and response-conflict monitoring. *Neuroimage, 20,* 1132–1139.

Garavan, H., Ross, T. J., Murphy, K., Roche, R. A. P., & Stein, E. A. (2002). Dissociable executive functions in the dynamic control of behavior: Inhibition, error detection, and correction. *Neuroimage, 17,* 1820–1829.

Ginsburg, A. P. (1986). Spatial filtering and visual form perception. In K. R. Boff, L. Kaufman, & J. P. Thomas (Eds.), *Handbook of perception and human performance, Vol. 2: Cognitive processes and performance* (pp. 1–41). Oxford: Wiley.

Gitelman, D. R., Penny, W. D., Ashburner, J., & Friston, K. J. (2003). Modeling regional and psychophysiologic interactions in fMRI: The importance of hemodynamic deconvolution. *Neuroimage, 19,* 200–207.

Grill-Spector, K. (2003). The neural basis of object perception. *Current Opinion in Neurobiology, 13,* 159–166.

Haxby, J. V., Gobbini, M. I., Furey, M. L., Ishai, A., Schouten, J. L., & Pietrini, P. (2001). Distributed and overlapping representations of faces and objects in ventral temporal cortex. *Science, 293,* 2425–2430.

Hegdé, J. (2008). Time course of visual perception: Coarse-to-fine processing and beyond. *Progress in Neurobiology, 84,* 405–439.

Hughes, H. C., Nozawa, G., & Kitterle, F. (1996). Global precedence, spatial frequency channels, and the statistics of natural images. *Journal of Cognitive Neuroscience, 8,* 197–230.

Hupé, J., James, A. C., Girard, P., Lomber, S. G., Payne, B. R., Bullier, J., et al. (2001). Feedback connections act on the early part of the responses in monkey visual cortex. *Journal of Physiology, 85,* 134–145.

Ishai, A., Ungerleider, L., Martrin, A., Schouten, J., & Haxby, J. V. (1999). Distributed representation of objects in the human ventral visual pathway. *Proceedings of the National Academy of Sciences, U.S.A., 96,* 9379–9384.

Kauffmann, L., Chauvin, A., Guyader, N., & Peyrin, C. (2015). Rapid scene categorization: Role of spatial frequency order, accumulation mode and luminance contrast. *Vision Research, 107,* 49–57.

Kauffmann, L., Ramanoël, S., & Peyrin, C. (2014). The neural bases of spatial frequency processing during scene perception. *Frontiers in Integrative Neuroscience, 8,* 1–14.

Kveraga, K., Boshyan, J., & Bar, M. (2007). Magnocellular projections as the trigger of top–down facilitation in recognition. *Journal of Neuroscience, 27,* 13232–13240.

Lerner, Y., Hendler, T., Ben-Bashat, D., Harel, M., & Malach, R. (2001). A hierarchical axis of object processing stages in the human visual cortex. *Cerebral Cortex, 11,* 287–297.

Mu, T., & Li, S. (2013). The neural signature of spatial frequency-based information integration in scene perception. *Experimental Brain Research, 227,* 367–377.

Musel, B., Chauvin, A., Guyader, N., Chokron, S., & Peyrin, C. (2012). Is coarse-to-fine strategy sensitive to normal aging? *PloS One, 7,* e38493.

Nee, D. E., Wager, T. D., & Jonides, J. (2007). Interference resolution: Insights from a meta-analysis of neuroimaging tasks. *Cognitive, Affective & Behavioral Neuroscience, 7,* 1–17.

Nelson, J. K., Reuter-Lorenz, P. A., Persson, J., Sylvester, C.-Y. C., & Jonides, J. (2009). Mapping interference resolution across task domains: A shared control process in left inferior frontal gyrus. *Brain Research, 1256,* 92–100.

Oliva, A., & Schyns, P. G. (1997). Coarse blobs or fine edges? Evidence that information diagnosticity changes the perception of complex visual stimuli. *Cognitive Psychology, 107,* 72–107.

Oliva, A., & Torralba, A. (2001). Modeling the shape of the scene: A holistic representation of the spatial envelope. *International Journal of Computer Vision, 42,* 145–175.

O'Reilly, J. X., Woolrich, M. W., Behrens, T. E. J., Smith, S. M., & Johansen-Berg, H. (2012). Tools of the trade: Psychophysiological interactions and functional connectivity. *Social Cognitive and Affective Neuroscience, 7,* 604–609.

Parker, D. M., Lishman, J. R., & Hughes, J. (1992). Temporal integration of spatially filtered visual images. *Perception, 21,* 147–160.

Peyrin, C., Baciu, M., Segebarth, C., & Marendaz, C. (2004). Cerebral regions and hemispheric specialization for processing spatial frequencies during natural scene recognition. An event-related fMRI study. *Neuroimage, 23,* 698–707.

Peyrin, C., Michel, C. M., Schwartz, S., Thut, G., Seghier, M., Landis, T., et al. (2010). The neural substrates and timing of top–down processes during coarse-to-fine categorization of visual scenes: A combined fMRI and ERP study. *Journal of Cognitive Neuroscience, 22,* 2768–2780.

Peyrin, C., Schwartz, S., Seghier, M., Michel, C., Landis, T., & Vuilleumier, P. (2005). Hemispheric specialization of human inferior temporal cortex during coarse-to-fine and fine-to-coarse analysis of natural visual scenes. *Neuroimage, 28,* 464–473.

Poggio, G. F. (1972). Spatial properties of neurons in striate cortex of unanesthetized macaque monkey. *Investigative Ophthalmology, 11,* 368–377.

Posner, M. I., & Petersen, S. E. (1990). The attention system of the human brain. *Annual Review of Neuroscience, 13,* 25–42.

Schyns, P. G., & Oliva, A. (1994). Evidence for time- and spatial-scale-dependent scene recognition. *Psychological Science, 5,* 195–201.

Shams, L., & von der Malsburg, C. (2002). The role of complex cells in object recognition. *Vision Research, 42,* 2547–2554.

Shomstein, S. (2012). Cognitive functions of the posterior parietal cortex: Top–down and bottom–up attentional control. *Frontiers in Integrative Neuroscience, 6,* 38.

Talairach, J., & Tournoux, P. (1988). *Co-planar stereotaxic atlas of the human brain. 3-Dimensional proportional system: An approach to cerebral imaging*. Stuttgart: Thieme.

Tanaka, K. (1996). Inferotemporal cortex and object vision. *Annual Review of Neuroscience, 19,* 109–139.

Thorpe, S. J., Fize, D., & Marlot, C. (1996). Speed of processing in the human visual system. *Nature, 381,* 520–522.

Van Essen, D., & Deyoe, E. A. (1995). Concurrent processing in the primate visual cortex. In M. Gazzaniga (Ed.), *The cognitive neurosciences* (pp. 383–400). Cambridge, MA: Bradford Book.

Volz, K. G., Schubotz, R. I., & von Cramon, D. Y. (2005). Variants of uncertainty in decision-making and their neural correlates. *Brain Research Bulletin, 67,* 403–412.

Wagner, A. D., Pare, E. J., Clark, J., & Poldrack, R. A. (2001). Recovering meaning: Left prefrontal cortex guides controlled semantic retrieval. *Neuron, 31,* 329–338.

Wais, P. E., Rubens, M. T., Boccanfuso, J., & Gazzaley, A. (2010). Neural mechanisms underlying the impact of visual distraction on retrieval of long-term memory. *Journal of Neuroscience, 30,* 8541–8550.

Yantis, S., Schwarzbach, J., Serences, J. T., Carlson, R. L., Steinmetz, M. A., Pekar, J. J., et al. (2002). Transient neural activity in human parietal cortex during spatial attention shifts. *Nature Neuroscience, 5,* 995–1002.